# EARTHQUAKE RESPONSE SENSITIVITY OF COMPLEX INFRASTRUCTURE NETWORKS

J. C. de la Llera(1,2,3), M. Monsalve(2,3), E. Ferrario(2,3), E. Allen(2,4), A. Chamorro(2,4), S. Castro(2), Y. Alberto(2,5), F. Arróspide(2), A. Poulos(2), G. Candia (2,6), P. Aguirre(2,3)

(1) Department of Structural and Geotechnical Engineering, Pontificia Universidad Católica de Chile; jcllera@ing.puc.cl
(2) Research Center for Integrated Disaster Risk Management (CIGIDEN), CONICYT/FONDAP/15110017; mauricio.monsalve@cigiden.cl, elisa.ferrario@cigiden.cl, eduardo.allen@cigiden.cl, sebastian.castro@cigiden.cl, alan.poulos@cigiden.cl
(3) School of Engineering, Pontificia Universidad Católica de Chile
(4) Department of Construction Engineering and Management, Pontificia Universidad Católica de Chile; achamorro@ing.puc.cl
(5) Department of Civil Engineering, University of Chile; yalberto@uchile.cl
(6) School of Engineering, Universidad del Desarrollo; gcandia@udd.cl

## *Abstract*

Resilience of complex infrastructure networks is critical in achieving earthquake resilience in urban environments. Perhaps due to their modeling complexity, very few research studies have addressed sensitivity of the network response to a severe earthquake hazard field. This research aims to characterize earthquake response sensitivity as a function of different topological parameters of 5 critical complex networks in central Chile, covering the electric, transportation, and drinking water networks. Central Chile was selected because it amounts for almost 50% of the country's population. What is also particular about this setting, is that the seismic characteristics of the region lead to extended (essentially) N-S strike fault ruptures, which run along the subduction margin defined by the E-W convergence between the South American and Pacific Ocean plates at an unusual rate of about 68 mm/year, thus involving in the strong-motion hazard field geographic scales in the hundreds of kilometers. It is concluded that node and link topological structures differ considerably between these complex systems, which are characterized by several different well-known centrality parameters and other interesting indices and network-class discriminators. Secondly, a component criticality analysis under an earthquake hazard field is also presented just in terms of connectivity/service loss, which enables, at least, a rough identification of the robustness of each network as nodes and links are removed. Results from these topological analyses are useful to identify which components are essential in generating larger earthquake resilience. This is the first time such results are obtained for central Chile using very detailed models of these complex networks.

*Keywords: complex infrastructure networks; earthquake resilience; centrality indicators; component criticality*

## 1. Introduction

This article summarizes some initial results of a large initiative aimed to study the performance of several networks in Central Chile as they are disrupted by extreme earthquake loading. The umbrella initiative is called SYBER-RISK[1], which is also part of the Research Center for Integrated Disaster Risk Management (CIGIDEN). Herein, information of several critical networks is presented, which by itself has archival value for future research, but the article also introduces a methodology to link the topological characteristics of these critical networks with the earthquake characteristics. For instance, the question of how do different centrality measures (topology) of these networks imply different sensitivity to earthquake loading, is central to our study.

Three of the networks considered are inner city networks: water, electricity and transportation, which are studied for the conurbation denoted as The Greater Valparaíso, specifically to the cities of Valparaíso, Viña del Mar and Concón. The two other networks are at regional scale, these are the interurban transportation

1 https://www.siberrisk.cl

system between the regions of Valparaíso and Santiago, as well as the complete electric transmission system for Chile. The idea in this research is to deal with different geographical scales to foresee different network topological parameters that may play later a fundamental role in risk and resilience analysis of these networks. Geometric and flow models for each of these networks have been developed based on public data; however, this article focuses exclusively on the topological component rather than the flow model, which is part of our future research.

The existing literature on the response of critical networks to earthquake loading is limited, but the more general literature on network component fragility is large [1][2][3][4]. Space limitations do not allow an extensive description of this previous work, but a good summary of the progress in the field may be found elsewhere [5]. The mathematical formulation of this problem is cast in terms of the typical risk analysis framework [5][6], which implies a consistent regional hazard model, a complete exposure and operational model of the network, a detailed description of the system fragilities in terms on different intensity measures (in this case due to subduction events), and the usual numerical Montecarlo computation scheme, which need in most practical cases the use of effective variance reduction techniques to improve simulation time.

On the other hand, network analysis is a consolidated field, which has done tremendous progress thanks to the rapidly increasing computational capacity that enables modeling and simulation of very complex systems [7][8][9][10]. This field, however, has not permeated well yet the earthquake engineering field, for which the latter still devotes strong efforts on the understanding of the seismic performance of individual structures rather than complex systems. Indeed, the former is required for the latter, but progress done in recent years in the estimation of the inelastic response of individual structures, justifies the need to start focusing also on the earthquake performance of complex networks, as a system, since their operations are critical for city earthquake resilience.

This article shows one step into that direction, and has not been absent of the usual complexities with the lack of proper information for complex system modeling. Some of this shortcomings are discussed herein, as well as the methodology employed to connect topological characteristics of these networks with the effects of subduction earthquakes acting on these networks. Different measures to characterize network topology have been used, and their basic characteristics explained. The application of these techniques to the networks considered serves as an example of the type of results possible to obtain and how could they be applied to improve resilience.

## 2. Methodology

The methodology employed in this research follows the classical risk analysis framework presented elsewhere [6]. However, given the space limitations of this article, larger emphasis is placed on the part of the methodology that is less known in the realm of earthquake engineering, leaving the details of the rest of the steps to the previous literature.

*Probabilistic Hazard Assessment*

The most significant characteristic of the Probabilistic Seismic Hazard Assessment (PSHA) is the need to characterize a random seismic field rather than earthquake Intensity Measures (IMs) at a given location. Models for the spectral and geographical correlations of IMs are then required, since each component of the system may be affected by more than a single IM, and different components of the network are spatially distributed on the territory. Conventionally, consistent vectors of correlated IMs are required for analyzing a network. In our case, the analysis considers nominally 30,000 scenarios, or less, which were generated previously [11] using importance sampling. For epicenter sampling, only earthquakes closer than 500 km of any component of the network were considered. The Ground-Motion Model (GMM) used was calibrated for a subduction zone [12] and incorporates site conditions through an average shear-wave velocity Vs30 derived from a global database of the USGS [13].

*Network topological analysis*



 

The idea behind this work is to study how the network topology affects the robustness of the selected infrastructure networks when the latter are subject to a seismic hazard. The methodology explores how the topological characteristics of the network elements, nodes and links, as they are removed by damage produced by the earthquake, impact the overall network connectivity. To do it, an experimental protocol was defined, which involves first to classify network elements according to four topological criteria: core/periphery, betweenness centrality, closeness centrality, and distance to a source (in hops or kilometers). These values are classified into categories of low or high, yielding a total of 16 combinations or classes.

Second, the networks are subject to 30,000, or less, previously defined seismic scenarios. Each of these (random field) scenarios, lead to a Peak Ground Acceleration (PGA) map, which consistently represents a vector of IMs for the different network components. Given the IMs at the location of the network components, different fragility functions were used to sample damage on the component. As a result of these fragility functions and sampling process, network elements might be removed (or not). After that, the number of nodes that become unreachable from the network source (water tanks, substations, etc.) was counted each time. A network source is a conceptual element of the network that is essential to its functionality. The number of unreachable elements leads to the so called outage size (blackout, severance) caused by the realization of the simulated earthquake.

Furthermore, the topological aspect is introduced by assessing the impact on the resulting outage size of removing types of elements in any of the 16 classes defined above. This is done by counting how many network elements of each class were removed for each earthquake scenario (realization), and by performing later a regression against the outage size. The particular type of regression performed was a simple nonnegative least squares linear regression without an intercept, i.e.

$$\text{argmax}_b \sum (b^T x_i - y_i)^2$$
$$\text{s.t. } b \geq 0$$

where $x_i$ is the vector of the number of removed elements of each class during the $i$-th realization; $y_i$ is the outage size induced in the $i$-th realization; and vector $b$ are the weighting coefficients given to each element class. From this regression, any coefficient $b_c$ indicates the sensitivity of the outage size to changes in an element of class $c$. Since this regression has no intercept, the outage size is explained solely by class removal counts.

*Betweenness and closeness centrality, core/periphery, and distance to a source*

The network parameters used to characterize the topology of the network relative to the importance of the nodes and likes are: (i) betweenness, and (ii) closeness centrality, (iii) core/periphery, and (iv) distance to a source. This section briefly describes these 4 metrics, and the reader is referred to the many excellent references in network analysis to a deeper explanation (e.g. [14]).

Betweenness centrality defines the importance of a node (or a link) in the communication of other pairs of nodes. It attempts to measure the portion of the information flow that goes through the given node in relation to the rest of the network. In its definition, it is assumed that the information goes from one node to another through the shortest path connecting them. The betweenness of node, or link $i$, in an undirected network is defined as:

$$B(i) = \sum \frac{\rho(j,k|i)}{\rho(j,k)}$$

where $\rho(j,k)$ is the number of shortest paths between nodes $j$ and $k$; and $\rho(j,k|i)$ is the number of shortest paths between $j$ and $k$ that pass through $i$; note that $i$ can be a node or a link.

The closeness centrality of node $i$ defines how close this node is from the rest of the nodes of the network. It is measured by the shortest path distance, i.e.,



 

$$C(i) = \frac{n-1}{\sum d\,(i,j)}$$

where $d(i,j)$ denotes the length of the shortest path from node $i$ to node $j$. In other words, closeness centrality is the multiplicative inverse of the average distance of node $i$ to the rest of the network. This definition can be easily extended to links and directed networks.

Betweenness and closeness centrality are metrics that rank nodes and links according to shortest paths and have been associated with network robustness [15]. As already explained, $B(i)$, measures how many shortest paths go through an element of the network, while closeness centrality, $C(i)$, is proportional to the inverse of the average shortest path length to the other elements in the network.

The core periphery structure of a network assumes that there are two classes of nodes, those that belong to a dense subnetwork in which the nodes are highly interconnected, and the rest of the nodes, which are a weakly connected to the core [16]. Ideally, core nodes are adjacent to other core nodes with some links to peripheral nodes, while peripheral nodes are weakly connected to other peripheral nodes. This requires a partition of the network that separates the nodes in core or peripheral.

The last metric of node relevance is the minimum path distance from the node to a source of the network. The shortest distance from a node to a source is relevant since it is assumed that if elements closer to a source are removed, the chances of having a near complete outage in the network increases. Sources for the electric transmission networks are power plants; for electric distribution systems are substations; for drinking water are water storage tanks; for urban road networks are the main exit or connections with other locations, and for interurban transportation networks are populated cities, or cities that may generate special and relevant traffic, say trucks, such as port cities.

## 3. Infrastructure networks considered

Five different networks were considered in the analysis, three are inner city networks and the other two are regional networks. The three inner city networks of The Greater Valparaíso area are: (a) the drinking water distribution network; (b) the medium voltage electric distribution network; and (c) the transportation network. The two regional networks are the: (d) interurban road network between the Valparaíso and Santiago regions; and (e) the national interconnected Electric Power Transmission Network of Chile. The geometry of these networks are presented in Figure 1; brighter segments depict sections closer to the identified network sources.

Table 1 briefly describes the elements of networks in terms of the classes of nodes, links, and other features such as sources and elements of the network that are seismically exposed. Please note that the definition of elements at risk depends on the resolution of the network. For instance, while substations correspond to the sources for the electric distribution network, they become elements at risk for the national electric transmission model. The definition of elements at risk is such that these are elements that may be removed, according to their fragility functions, from the network during the analysis.

Table 1 – Descriptive summary of the five networks considered.

| Network | Links | Nodes | Sources | Elements at risk |
|---|---|---|---|---|
| Water distribution; Greater Valparaíso | Pipes | Pipe junctions, water reservoirs, elevation plants | Water reservoirs, elevation plants | Pipes |
| Electric distribution-- Mid voltage; Greater Valparaíso | Overhead line segments | Electric poles, towers, distribution substations | Distribution substations | Overhead lines |
| Transportation network; Greater Valparaíso | Street segments (1-block length) | Intersections, dead-ends, highwat exits | Highway exits | Street segments |



 

| | | | | |
|---|---|---|---|---|
| Interurban network, Valparaíso and Santiago regions | Roadways between nodes | Road junctions, city exits | Most populated cities: Santiago, Great Valparaíso, and San Antonio | Roadways, tunnels and bridges |
| National Electric System of Chile (transmission) | Lines between substations | Substations | Substations associated with generation plants | Substations |

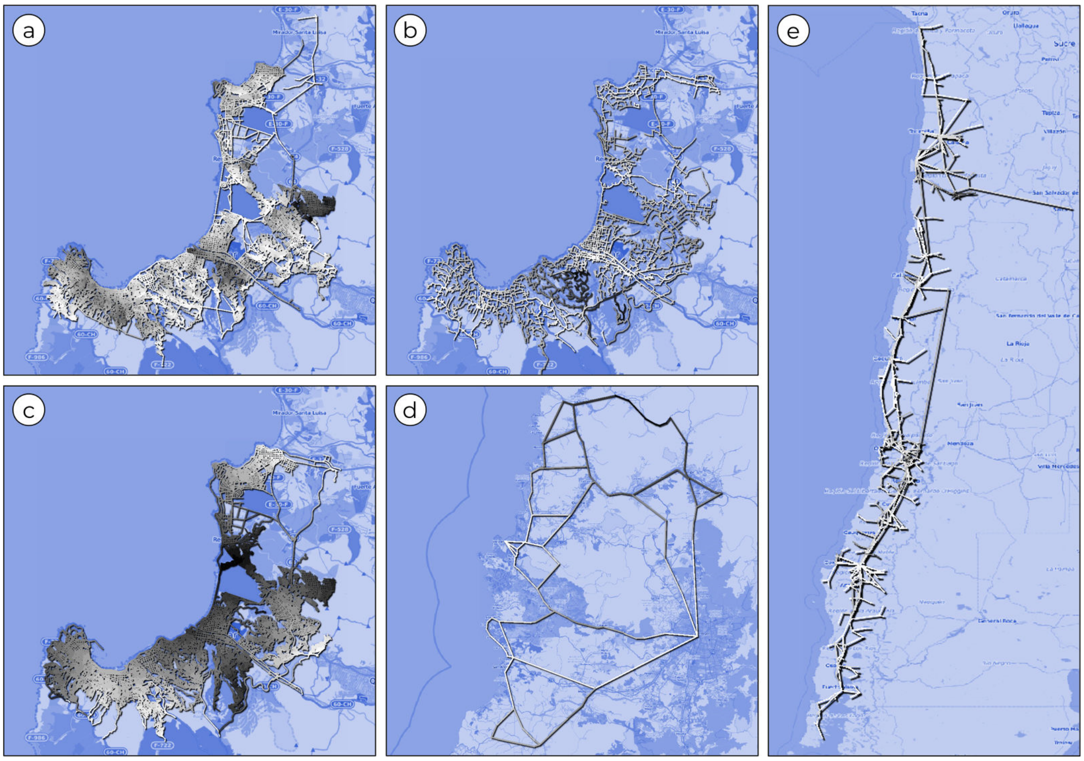


Fig. 1 – Models of the five networks considered, cases (a), (b) and (c) correspond to The Great Valparaiso area, while (d) and (e) are regional ones: (a) drinking water network; (b) electric distribution network; (c) urban transportation network; (d) interurban transportation network; and (e) electric power transmission network.

*Drinking water distribution network*

The water distribution network for The Greater Valparaíso area comprises 39778 links and 36403 nodes. The network was constructed from data requested to the Superintendence of Sanitary Services (SISS) and was manually and automatically corrected until the complete water distribution was properly functional. Although only connectivity information has been considered in this research, the data has been curated for hydraulic analysis with the EPANET software.

Drinking water is provided to the rest of the network through water tanks and elevation stations (pumping stations or boosters), which are located in the hills inside the conurbation. These are the network sources. Then, this water reaches consumers through a network of pipes, because of gravity. These pipes comprise a variety of materials and diameters, however, this work is only concerned with connectivity.

The elements considered at risk in this case were the pipelines themselves; it was assumed that the rest of the components of the network could not undergo damage. This is a simplification, but in general most of the damage observed in these networks occurs in the pipelines. The fragility curve for the pipes is illustrated in Figure 2. Additional data for informing the fragility curves, such as pipe material and diameter as well as soil type and slope, were ignored in this analysis, and will be the subject of future work.



 

*Electric distribution network*

The data for the electric distribution network of The Greater Valparaíso Area was collected exclusively from online sources, as described in previous work [17]. This work focuses only on the medium voltage subnetwork, which consists of 24954 links and 24610 nodes. The retrieved data consisted of map drawings (GIS vector data), so there were some geometric imperfections, which prevented a direct translation of the line segments into links and edges. Therefore, automated correction rules were used to patch this data and ensure all nodes have a path to the network sources (the substations).

The electric distribution network takes the electricity provided by the electric transmission network (also considered in this work), which is supplied from the substations to the conurbation. These substations are the network sources. This electricity is distributed to the city through a network of medium voltage overhead lines, which hang from utility poles. Medium voltage is converted to low voltage through transformers, allowing it to reach an even larger extent of consumers through differentiated overhead lines. This work, however, only models medium voltage distribution, independent of the transmission network.

The elements considered at risk in this case are the overhead lines, whose fragility curves were obtained earlier [18]. These fragility functions are also presented in Figure 2, and are used to determine when electric lines may collapse as a result of a given earthquake intensity.

*Inner city transportation network*

The inner city transportation network of The Greater Valparaíso conurbation was also considered in this work. This network comprises the streets and avenues in the conurbation, and is limited by the highway exits. The network provides access to people and businesses to the varied services located throughout the conurbation and beyond, and in this model, highway exits were classified as network sources.

This network comprises 30944 links and 25952 nodes. Streets were considered as links, while intersections, dead-ends, and highway exits were considered as nodes. The elements at risk of this network were the streets themselves; however, in absence of a proper fragility curve for streets, a variation of the fragility curve for 2-lane highways was used (see the inter-urban network and Figure 2). In particular, it was assumed for this fragility that a 2-lane highway was in average 50 times longer than a city street. Then, if $f_{2L}(\text{pgd})$ is the fragility curve of a 2-lane highway, the fragility curve assumed for the street is

$$f_{street}(\text{pgd}) = 1 - \left(1 - f_{2L}(\text{pgd})\right)^{1/50}.$$

*Inter-urban transportation network*

The national road network, Route 5, runs for about 3.000 km north to south and is the main longitudinal road of the country. It connects with several transversal routes (east-west) that interconnect the mountains on the east with the Pacific coast on the west. Densification policies of the road network have been developed in the last 20 years; this has brought in some territories larger fragilities due to the morphological conditions. The analyzed infrastructure assets correspond to roads (2-lane highways and multi-lane highways), tunnels, and bridges for the specified routes.

Nodes were defined at road intersections and at the beginning or end of a specific infrastructure within a route such as a tunnel or bridge. Bridges generate two nodes, one node at the beginning and another at the end. Links are defined as roads, bridges, and tunnels and contain all geometric properties of the link and information such as seismic fragility, flow capacity, and design velocity. The network considers 159 nodes and 173 links distributed in 6 tunnels, 59 bridges, 62 two-lane highways, and 46 multi-lane highways.

Seismic fragility models used in this study consider only severe damage, and were developed by different authors and are summarized in Figure 2 for bridges, tunnels, multi-lane and two-lane highways [19][20][21]. The models adopted in the study consider Permanent Ground Displacement (pgd) as the intensity measure, which is calculated based on the methodology first proposed in [22]. The methodology to estimate expected pgd is based on the liquefaction susceptibility and the PGA for the specific site. Although, each damage state leads to different conditions in terms of traffic capacity for each type of infrastructure, only the severe/complete damage state was considered for connectivity analysis.

*National electric transmission network*

The national electric transmission network essentially covers all the country, from the northernmost region of Chile to the Chiloé Island in the south. It has an extension of 3100 km and serves the 98.5% of the Chilean population. This network was reconstructed from the data available from the National Electrical Coordinator [23], and from other official Chilean sources such as the Ministry of Energy [24], and the National Energy Commission through its Energía Abierta platform [25]. All databases were used to complement or correct data.

In general, the electric power transmission system is mainly composed by power plants, substations, transmission lines and loads. However, given that this work focuses on network topology, only substations and transmission lines, representing nodes and links, respectively, are considered. Substations connected to a power plant are identified as source nodes. In total, the system under analysis is composed by 994 substations, with 274 source nodes and 1195 transmission lines. A detailed description of the Chilean electric transmission network model is provided in [26], together with the main difficulties encountered in the model construction.

The elements considered at risk in this case are the substations. Seismic fragility curves of substations are taken from [27], where a distinction is made for anchored facilities with low (between 34.5 kV and 150 kV), medium (between 150 kV and 350 kV), and high (above 350 kV) voltage substations. For each facility, different fragility curves for different levels of damage (minor, moderate, extensive and complete) are provided elsewhere [27]. In this work, it is assumed that a substation that enters in any level of damage shuts down operationally. Then, the fragility curve corresponding to the minor damage level is here adopted as a conservative estimate (Figure 2). When a substation fails to operate, all lines connected to it are removed from the network.

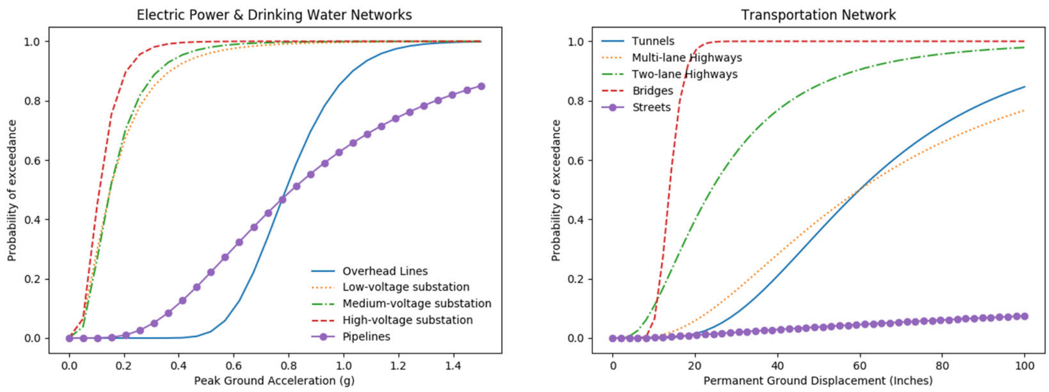


Fig. 2 – Fragilities considered in this work. The left inset shows all the fragility curves associated with peak ground acceleration (PGA), while the right inset shows the fragility curves associated with permanent ground displacement (pgd).

## 4. Research results

The number of Montecarlo simulations required varied among systems (for network (a) ≡ 14718, and 30,000 for the rest). These simulations were used to compute the different topological indices already described for the five networks considered. Table 2 summarizes descriptive statistics for each of the networks, which are specified by the names in each row.

It is also interesting to visualize the networks when they are in absence of their spatial layout (Figure 3). This visualization enables a better understanding of some of the topological features of each network. Rendering of the networks was done using a stress minimization algorithm called distance scaling [28], in which the visual distance of the nodes aims to match their shortest path distance. This rendering produces network visualizations that are well spread, preventing unnecessary overlaps of links or nodes.



 

Table 2 – Topological features of the five networks considered: (a) drinking water network; (b) electric distribution network; (c) urban transportation network; (d) interurban transportation network; and (e) electric power transmission network.

| Network | # Elements | Degree(*) | Distance to a source (hops) | Betweenness | Closeness | Core size |
|---|---|---|---|---|---|---|
| Water distribution; Great Valparaíso | 39778 links<br>36403 nodes | Median: 2<br>Average: 2.19<br>Maximum: 8 | Median: 32<br>Average: 36.1<br>Maximum: 138 | Median: 0.000258<br>Average: 0.00577<br>Maximum: 0.458 | Median: 0.00486<br>Average: 0.00486<br>Maximum: 0.00647 | 1419 |
| Electric distribution--Mid voltage; Great Valparaíso | 24954 links<br>24610 nodes | Median: 2<br>Average: 2.03<br>Maximum: 8 | Median: 99<br>Average: 117.7<br>Maximum: 496 | Median: 0.00037<br>Average: 0.004<br>Maximum: 0.105 | Median: 0.00145<br>Average: 0.00147<br>Maximum: 0.00259 | 198 |
| Transportation network; GreatValparaíso | 30944 links<br>25952 nodes | Median: 2<br>Average: 2.39<br>Maximum: 8 | Median: 92<br>Average: 91.1<br>Maximum: 194 | Median: 0.000453<br>Average: 0.00687<br>Maximum: 0.321 | Median: 0.00567<br>Average: 0.0057<br>Maximum: 0.00824 | 3122 |
| Interurban network, Valparaíso and Santiago regions | 173 links<br>158 nodes | Median: 2<br>Average: 2.19<br>Maximum: 4 | (in km)<br>Median: 51.5<br>Average: 53.1<br>Maximum: 128.2 | Median: 0.0963<br>Average: 0.107<br>Maximum: 0.354 | Median: 0.0694<br>Average: 0.07<br>Maximum: 0.09 | 76 |
| National Electric System of Chile (transmission) | 1195 links<br>994 nodes | Median: 2<br>Average: 2.4<br>Maximum: 33 | Median: 1<br>Average: 1.48<br>Maximum: 7 | Median: 0.002<br>Average: 0.03<br>Maximum: 0.454 | Median: 0.083<br>Average: 0.084<br>Maximum: 0.137 | 155 |

(*)Degree: the degree of a node is the number of links in which it participates.

Shown in Figure 4 are the simulation results. Each inset depicts the number of removed elements in the *x*-axis and the number of unreachable elements in the *y*-axis. The insets represent the: (a) drinking water distribution network; (b) medium voltage electric distribution network; (c) street network; (d) inter-urban road network; and (e) national electric transmission network. With the exception of the latter inset (e), most models show similar behavior between the number of removed links and the number of unreachable nodes. Roughly, when about ¼ of the links are removed, most of the nodes become unreachable and the collapse of the network is complete. The behavior of the electric power transmission network shows that the system is quite robust from the seismic perspective since a phase change in the connectivity is not apparent.

Essentially, all components (nodes and links) were classified by their topological characteristics, i.e., distance to the source measured in link hops or in miles (transmission, highways); Betweenness centrality, measured by how many shortest paths go through the element (node or link); Closeness centrality, measured by the average proximity to the rest of the network; and Core/periphery—in which rich-club analysis assumes that networks experience well connected cores (the rich club) and other poorly connected elements (the periphery), which can have access to the rest of the network only through the core. In our analysis, nodes and links were classified and labeled by having high or low distance, betweenness, and closeness, and whether they belong to the core or the periphery of the network. High or low values were determined relative to the score being above or below the median value for all nodes, respectively.


 

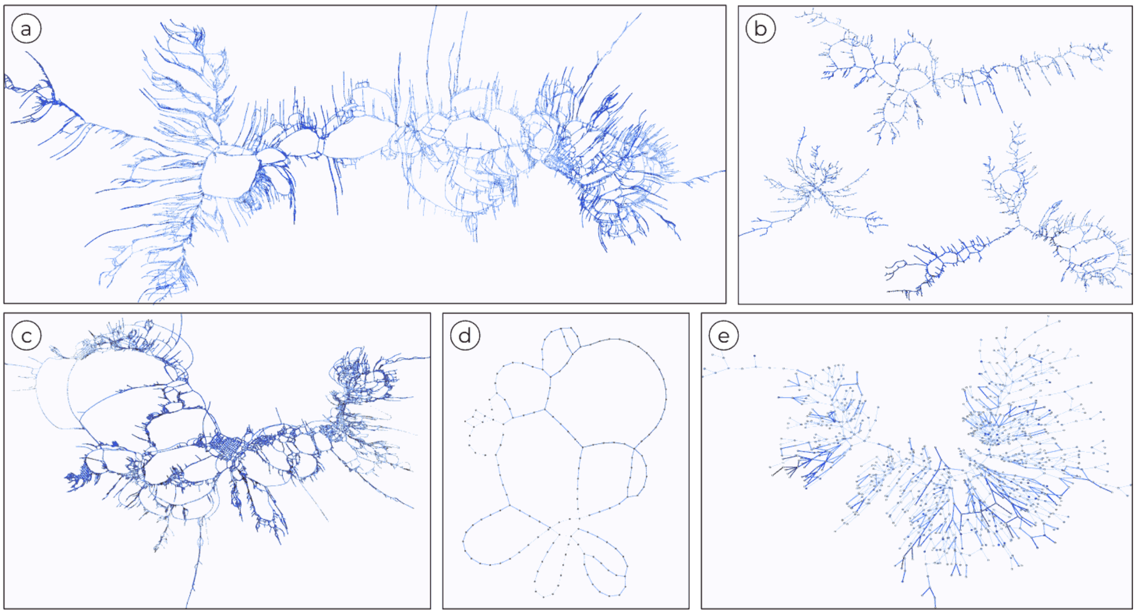


Fig. 3 – Network visualization in absence of the geographical setting: (a) water distribution network; (b) electric distribution network; (c) inner-city transportation network; (d) inter-urban transportation network; and (e) national electric transmission network of Chile.

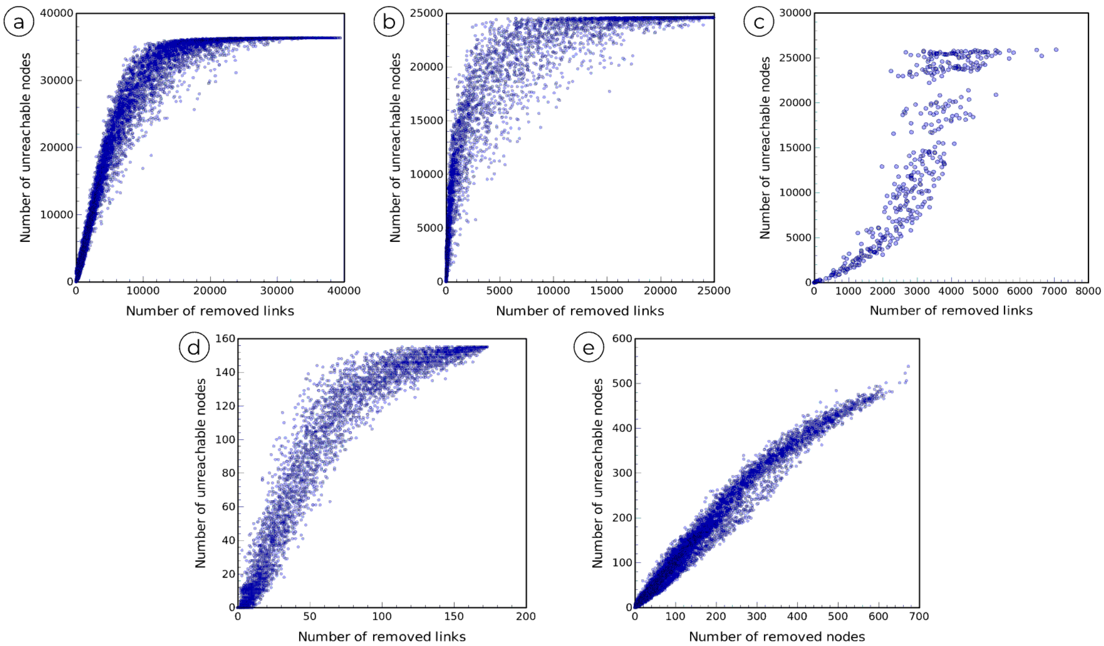


Fig. 4 – Simulation results that relate the number of removed links due to earthquake damage and the number of unreachable nodes for the different networks: (a) water distribution network; (b) electric distribution network; (c) inner city transportation network; (d) inter-urban transportation network; and (e) national electric transmission network.

In order to relate the topological characteristics of each element with the impact of the earthquake realization on the connectivity of the network, a table with the sample structure shown in Table 5 was produced for each network. Apart from the number in the first column that denotes the realization number, the number shown in each cell of the table reflects the number of elements that fall in the category defined by the column label for each realization. Thus, to assess the impact of removing elements of the network based on their topological characteristics, a regression was performed on the results of an equivalent of Table 5 for each network. The regression used was a nonlinear least squares since the contribution of the removal of an element to the outage size can never be negative.

Based on these tables, the regression results are summarized in Figure 5. Classes refer to any link or node associated with the column labels in Table 5, which define a combination of the different topological features and the intensity of the expression of that feature, high or low. The bar charts in the figure represent the coefficients of the *b* vector obtained in the nonnegative regression. For each element class and network, the value obtained indicates how many nodes are added to the resulting outage if an element of the class is removed. At first glance, it can be inferred that in the sparser networks (water and electric distribution), element importance is concentrated in a few classes, while in the more redundant networks, element importance is more distributed among classes. In general, it is apparent that removing elements from the core induces larger outages than removing peripheral elements.

Table 5 – Example of the classification of network elements according to the topological characteristics chosen for each of the 16 possible categories defined; a table like this is generated for each network

| Simulation id | Core<br>High Betweenness<br>High Closeness<br>Close to the source | Core<br>High Betweenness<br>Low Closeness<br>Far from the source | Periphery<br>High Betweenness<br>Low Closeness<br>Close to the source | ... | Unreachable elements |
|---|---|---|---|---|---|
| 1 | 0 | 1 | 5 | ... | 16 |
| 2 | 0 | 0 | 0 | ... | 0 |
| 3 | 0 | 5 | 12 | ... | 89 |
| ... | ... | ... | ... | ... | ... |

In the water distribution network, the removal of high betweenness centrality links in the core of this network brings the greatest loss of connectivity, especially when the links also have high closeness centrality. However, since the periphery of this network is so big, most of the disconnections are explained by the loss of links in the periphery.

In the electric distribution network, by far the most critical links are those in the core that have high betweenness and high closeness. These links are always close to the sources, where the core lies. Periphery and low betweenness links explain most of the blackouts, while high betweenness links generally appear to contribute very little to blackout sizes.

The inner-city transportation network is characterized by the presence of several alternative paths between origins and destinations. In this network, the most critical links are of two types. If they are in the network core, critical links are far from the source and have high closeness centrality and low betweenness; and if they are in the periphery, critical links are close to the source and have high closeness and betweenness centralities.

The inter-urban transportation network exhibits great redundancy of paths, so link importance is well distributed among link classes. Still, removing high betweenness links in the core seem to contribute the most to disconnect nodes from the sources (highly populated cities).

Finally, in the national electric transmission network, importance was given to nodes instead of links, because seismic affectation was modeled for nodes (substations). This network exhibits a good amount of path redundancy. Because of this, most node classes contribute significantly to blackout sizes. The most critical nodes, however, are those in the core that have high betweenness and low closeness centrality.

## 5. Conclusions

This work presented some preliminary results in the analysis of several infrastructure networks of Chile subject to severe seismic loads, from a topological (connectivity) viewpoint. Three types of services were covered: drinking water distribution, electricity supply, and transportation. The networks spanned different geographic levels, from the urban level (The Greater Valparaíso conurbation) to the national level.

The analysis presented herein assessed how many network elements were left without service when a link or node was removed based on its characteristics as a result of the earthquake intensity. This analysis was not limited to a single element removal, but to several elements as a consequence of simulated earthquake scenarios causing, sometimes, massive outages (blackouts). In general, it was found that removing elements from the network core, the well-connected portion, increase outages more than removing peripheral links or nodes. This could preliminary guide network investments to improve resilience.

Future work will consider more realistic network information with better resolution and improved data curation; the network models presented herein are still simple and their full functionality should be explored from a network under real seismic conditions. Interdependencies between infrastructures should be considered in future work as well. The regression analysis presented should also be improved to better represent the nonlinear relation between link or node removal and outage size.

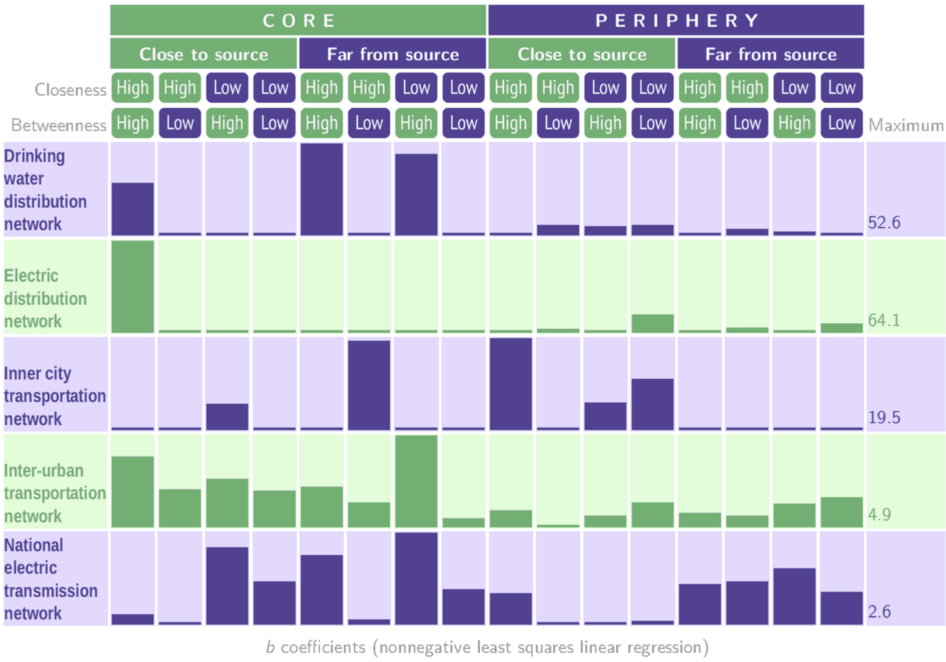


Fig. 5 – The contribution to outage size of removing a network element (link or node) according to its topological characteristics for each of the studied networks. Element importance was obtained from the *b* coefficient resulting from the regression. The topological characteristics of each element class are shown at the top. The bar charts are proportional within a network; the score of the maximum value for each network is shown to the right.

## 6. Acknowledgements

This research has been sponsored by the Research Center for Integrated Disaster Risk Management (CIGIDEN), CONICYT/FONDAP/15110017, as well as CONICYT/FONDECYT/1170836 "SIBER-RISK: Simulation Based Earthquake Risk and Resilience of Interdependent Systems and Networks"; Fondef Project ID14I20309, "Research and Development of Models to Quantify and Mitigate the Risk of Natural Hazards in the National Road Network"; CONICYT/FONDECYT/1181754, "Socio-economic modeling of mitigation strategies for resilient critical infrastructure: Application to drink water systems and road networks"; and postdoctoral Fondecyt grants CONICYT/FONDECYT/3180464, "Risk Analysis for Critical Infrastructures Protection", and CONICYT/FONDECYT/3170867, "Modeling the impact of natural hazards on complex interdependent systems using multilayer networks and graphical models".

## 7. References

**[1]** Tsinidis, G., Di Sarno, L., Sextos, A., & Furtner, P. (2019). A critical review on the vulnerability assessment of natural gas pipelines subjected to seismic wave propagation. Part 1: Fragility relations and implemented seismic intensity measures. Tunnelling and Underground Space Technology, 86, 279-296.



 

**[2]** Muntasir Billah, A. H. M., & Shahria Alam, M. (2015). Seismic fragility assessment of highway bridges: a state-of-the-art review. Structure and Infrastructure Engineering, 11(6), 804-832.
**[3]** Nair, G. S., Dash, S. R., & Mondal, G. (2018). Review of Pipeline Performance during Earthquakes since 1906. Journal of Performance of Constructed Facilities, 32(6), 04018083.
**[4]** Faturechi, R., & Miller-Hooks, E. (2015). Measuring the performance of transportation infrastructure systems in disasters: A comprehensive review. Journal of infrastructure systems, 21(1), 04014025.
**[5]** Fragiadakis, M., Vamvatsikos, D., Karlaftis, M. G., Lagaros, N. D., & Papadrakakis, M. (2015). Seismic assessment of structures and lifelines. Journal of Sound and Vibration, 334, 29-56.
**[6]** McGuire, R. K. (2004). Seismic hazard and risk analysis. EERI Monograph, MNO-10, Earthquake Engineering Research Institute.
**[7]** Albert, R., & Barabási, A. L. (2002). Statistical mechanics of complex networks. Reviews of modern physics, 74(1), 47.
**[8]** Brummitt, C. D., D'Souza, R. M., & Leicht, E. A. (2012). Suppressing cascades of load in interdependent networks. Proceedings of the National Academy of Sciences, 109(12), E680-E689.
**[9]** Yang, Y., Nishikawa, T., & Motter, A. E. (2017). Small vulnerable sets determine large network cascades in power grids. Science, 358(6365), eaan3184.
**[10]** D'Souza, R. M., Gómez-Gardeñes, J., Nagler, J., & Arenas, A. (2019). Explosive phenomena in complex networks. Advances in Physics, 68(3), 123-223.
**[11]** Poulos, A., Monsalve, M., Zamora, N., & de la Llera, J. C. (2019). An Updated Recurrence Model for Chilean Subduction Seismicity and Statistical Validation of its Poisson Nature. Bulletin of the Seismological Society of America, 109(1), 66-74. doi:10.1785/0120170160
**[12]** Abrahamson, N., Gregor, N., & Addo, K. (2016). BC Hydro ground motion prediction equations for subduction earthquakes. Earthquake Spectra, 32(1), 23-44.
**[13]** Allen, T.I., Wald D.J. (2017). Topographic Slope as a Proxy for Seismic Site-Conditions (VS30) and Amplification Around the Globe. U.S. Geological Survey Open-File Report 2007-1357, Reston, Virginia.
**[14]** Barabási A.L. Network Science. Cambridge University Press. 2016.
**[15]** Iyer S, Killingback T, Sundaram B, Wang Z. Attack robustness and centrality of complex networks. PLoS One. 2013;8(4):e59613. https://doi.org/10.1371/journal.pone.0059613
**[16]** Ma A, Mondragón RJ (2015) Rich-Cores in Networks. PLOS ONE 10(3): e0119678. https://doi.org/10.1371/journal.pone.0119678
**[17]** Monsalve M, de la Llera JC. Identifying Critical Components in Power Distribution Networks using Graph Theoretical Measures. 29th European Safety and Reliability Conference (ESREL 2019). Hannover, Germany, September 22-26, 2019.
**[18]** Vanzi I. 1996. Seismic reliability of electric power networks: methodology and application. Structural Safety 18(4): 311-327.
**[19]** Basoz, N., & Mander, J. (1999). Enhancement on the Highway Transportation lifeline module in Hazus, National Institute of Building Sciences, Draft 7.
**[20]** G&E Engineering Systems, Inc. (1994). NIBS Earthquake Loss Estimation Methods, Technical Manual, Transportation Systems (Highway Systems).
**[21]** National Institute of Building Sciences (NIBS) (2004). HAZUS-MH: users's manual and technical manuals. Report prepared for the Federal Emergency Management Agency, Washington, DC
**[22]** Joyner, W. B., & Boore, D. M. (1988). Measurement, Characterization, and Prediction of Strong Ground Motion, Proceedings of Earthquake Engineering & Soil Dynamics II, pp. 43- 102. Park City, Utah, 27 June 1988. New York: Geotechnical Division of the American Society of Civil Engineers.
**[23]** Coordinador (2019b). https://infotecnica.coordinador.cl/ Coordinador Eléctrico Nacional. Last Access March 2019.
**[24]** Ministry of Energy (2019) sig.minenergia.cl/sig-minen/moduloCartografico/composer/ Ministerio de Energía. Last Access March 2019.
**[25]** Energía Abierta (2019). http://energiaabierta.cl/ Energía Abierta. Last access March 2019.
**[26]** Ferrario E., Poulos A., de la Llera J. C., Lorca A., Oneto A. and Magnere C. Representation and Modeling of the Chilean Electric Power Network for Seismic Resilience Analysis. 29th European Safety and Reliability Conference (ESREL 2019). Hannover, Germany, September 22-26, 2019.
**[27]** FEMA (2003). Hazus-MH 2.1 Technical Manual. Department of Homeland Security, Federal Emergency Management Agency, Mitigation Division Washington, D.C.
**[28]** Brandes, U., & Pich, C. (2008, September). An experimental study on distance-based graph drawing. In International Symposium on Graph Drawing (pp. 218-229). Springer, Berlin, Heidelberg.



 